

the monosaccharides into carbon dioxide, hydrogen, and volatile fatty acids (VFAs), such as butyric acid. The third step is acetogenesis, where the VFAs are degraded into acetate. The final step is methanogenesis, where the acetate degrades into methane and carbon dioxide (Deng, Liu, and Wang 2020).

AD is a biochemical reaction completed by cooperation of different microorganisms. Each process of AD is represented and accompanied by chemical reactions. Since these reactions are either endothermic or exothermic, thus it is expected a considerable amount of heat exchange will occur, resulting in temperature differences that produce natural convection currents that redistribute ecosystem microorganisms, generating a new heat generation or absorption map (Zobaa and Bansal 2011).

Recently, the authors investigated the effect of the size and surface area of the digester parameters on the performance of anaerobic digestion, as dealing with Nasir et al. (2015) and Ogunwande and Akinjobi (2017), respectively. Therefore, their results showed that the size and surface area (height-to-diameter ratio of the digester) directly affect the gas production quantity.

Also, the authors investigated factors for high-efficient AD performance. Li, Jha, and Bajracharya (2014), Rathaur et al. (2018), Rajput, Zeshan, and Hassan (2021), Noonari et al. (2020) and Erdiwansyah et al. (2022) focused on the improvisation of biogas production quantity and quality from other co-digestion wastes with their mixtures. Komemoto et al. (2009) examined the effect of temperature on the solubilization and acidogenesis of food waste. Rodríguez, Pérez, and Romero (2013) used the organic portion of municipal solid waste as feedstock under mesophilic (35 °C) and thermophilic (55°C) conditions to evaluate the specific growth rate of microorganisms. Fedailaine et al. (2015) developed a mathematical model based on biomass mass balances to simulate anaerobic digestion.

Some authors investigated the anaerobic digester's performance by utilising computational fluid dynamics (CFD) to study the mixing behaviour of the fluid flow, energy, and chemical reactions and their effect on anaerobic digestion. Meroney and Colorado (2009) and Terashima et al. (2009) simulated sludge mixing characteristics and properties for full-scale different circular anaerobic digester tanks producing biogas. Leonzio (2018) and Saini et al. (2021) established the best geometrical configuration for a mixing system (mechanical mixing and automated sludge circulation) to save the power used in anaerobic digestion. Wu, Bibeau (2009) analyzed the reaction rate's influence on biogas production for a plug flow anaerobic digester. Wu (2010a) ; Wu (2010b) evaluated twelve turbulence models of a 3D single-phase and multiphase non-Newtonian fluid flow in anaerobic digesters for horizontal pipe by comparing the frictional pressure obtained from CFD with those from a correlation analysis for effective mixing improvement.

Bridgeman (2012), Shen et al. (2013), Mohammadrezaei, Zareei, and Khazaei (2018), and Chen et al. (2019) determined suitable loading sludge, a suitable mixing speed, appropriate blade type, the appropriate number of impellers and evaluated the optimal mechanical mixing method for biogas generation enhancement of anaerobic digester. Martínez et al. (2011), Conti, Saidi, and Goldbrunner (2019) and Dabiri et al. (2021) identified dead zones, established the best geometrical configuration, evaluated the mixer energy consumption and velocity gradient to ensure the highest sludge mixing efficiency inside the full-scale anaerobic digester. Kamarád et al. (2013), Dapelo and Bridgeman (2018) and Mao et al. (2019) investigated the minimum retention time of the fed substrate with different mixing systems for real large-scale anaerobic digesters. Patricia et al. (2020) and El Ibrahimy et al. (2021) studied and analysed the influence of heating and liquid recirculation on digesters with submerged wastes under mesophilic conditions on the thermodynamic performance of the digester. Acetogenesis and methanogenesis reactions were studied by Azargoshasb et al. (2015) using 3D CFD and population balance

equations. They used the Eulerian multiphase and $(k - \epsilon)$ turbulence models to simulate the reaction in hydrodynamics in a reactor with various influent VFA concentrations and hydraulic retention durations (HRT).

Rezavand et al. (2019) developed a 2D entirely Lagrangian computational model to combine mixing and biological response in anaerobic digestion. The diffusion equation provides the mass transfer interactions between the particles to link mixing to biochemical reactions. Using a multiphase CFD model, Jegede et al. (2020) evaluated an optimized Chinese dome digester, and the findings were compared to the results of pilot-scale trials. The self-agitation cycles are characterized by steady and improved hydraulic properties and mixing in the designed digester. Zarei et al. (2021) described the hydrodynamic regime of flow and mass transfer of species within the lab scale continuous packed bed with a multi-sized distributed particles bioreactor, and the anaerobic methanogenesis reactions occur at the particle surfaces.

From the literature above, and to our knowledge, the influence of different horizontal circular extended surfaces around the inside of the batch household digester on the biogas-producing efficient performance has not been previously researched. However, there is little effort to increase surface area without using extended surfaces, such as the work of Nasir et al. (2015) and Ogunwande and Akinjobi (2017). The objective of this paper is to fill this gap by building a 3D axisymmetric model for a batch digester based on the fundamental equations of conservation (mass, momentum, energy, and transport of diluted species) and the fundamentals of the four stages of the biochemical processes of AD (hydrolysis, acetogenesis, acetogenesis and Methanogenesis) using cow dung as the substrate to analyse and determine the effects of the reaction rate, the heat source, and the natural convection from the extended surfaces for improving the quantity and quality of biogas production.

2. CFD MODEL

2.1 Geometry and Principle of Operating

The simulations and modelling were performed on four batch digesters (D1, D2, D3, and D4) fabricated from PVC materials with a volume of 13 L (24 cm in diameter and 30 cm in height). The active working of each digester was at a 22 cm height (75 % working volume) filled with wet cow manure and water at a mixing ratio of 1 kg: 1 L, respectively. The released biogas accumulated in the residual part above the slurry. The horizontal circular PVC extended surface areas were equipped with the four batch digesters, with D1 having no extended surfaces. D2, D3, and D4 were provided with extended surfaces with widths of 2, 4, and 6 cm, respectively. Four layers were distributed prime from below, one of each 5 cm in height for the digester. The geometries of these 3D axisymmetric digesters were developed using the commercial COMSOL 5.5 Multiphysics software, as shown in Fig. 2.

2.2 Assumptions for Developed CFD Model

AD is a complex process composed of many physical, chemical, and biological sub-processes. The AD modelling is governed by the conservation of mass, momentum, energy, and species transport equations integrated with the biochemical reactions model. The following assumptions are required for the developed model:

- Carbohydrates decompose into glucose (monosaccharides) in the hydrolysis process.
- Glucose is metabolized into butyric acid (a VFA) in the acidogenesis process.
- Butyric acid is degraded into acetic acid (acetate) during the acetogenesis process.

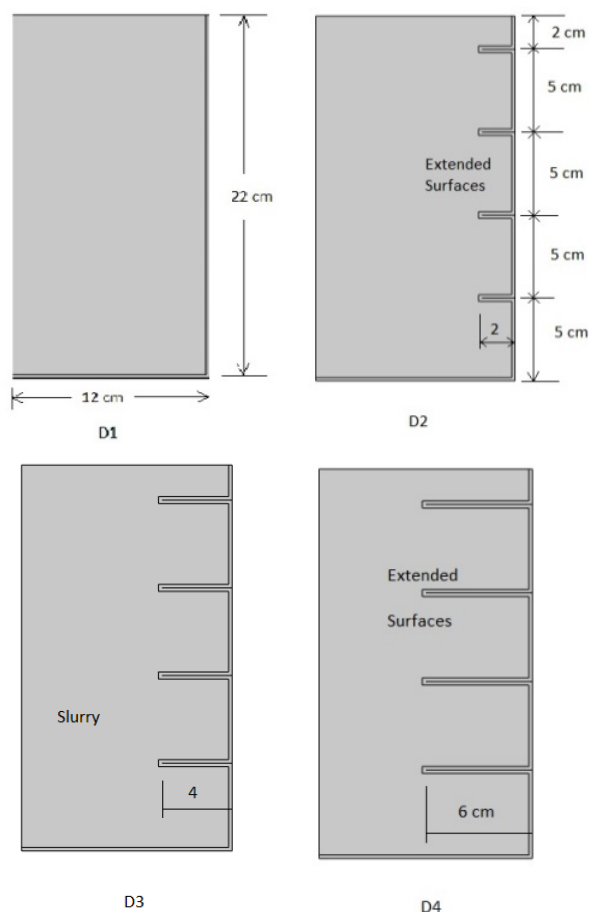


Fig. 2 The geometry of the 3D axisymmetric of the digesters shows extended surfaces.

- Methane and carbon dioxide are formed from acetic acid in the methanogenesis process.
- The model is 2D axisymmetric.
- The model is time-dependent.
- The run time is thirty days and seven days for each process except for methanogenesis, which takes nine days.
- The gravity, reduced pressure, and Boussinesq approximation are included in the fluid flow.
- The manure is single phase and phase interaction negligible.
- The generated biogas is released above the surface and does not affect the liquid manure.
- The outside walls of the digesters are adiabatic.
- The viscose dissipation is negligible.

2.3 Mathematical Model

The mathematical model includes the CFD equation solutions numerically based on the conservation laws using the commercial COMSOL 5.5 Multiphysics software code which simulates the AD in the batch digester with two multiphysics: the non-isothermal flow (laminar flow and heat transfer in fluid) and the engineering reactions (chemistry and transport of diluted species).

- Laminar flow: the behaviour of the liquid manure velocity in the digesters is governed by the momentum equation given by equation (1), which, coupled with the flow continuity equation, is provided by equation (2).

$$\rho \frac{\partial u}{\partial t} + \rho(u \cdot \nabla)u = \nabla \cdot [-pI + \mu(\nabla u + (\nabla u)^T)] + (\rho - \rho_{ref})g \quad (1)$$

$$\rho \nabla \cdot u = 0 \quad (2)$$

u is the flow velocity (m/s), p is the local pressure (Pa), I is the unit tensor, ρ is the fluid density (kg/m³), μ is the dynamic viscosity of the fluid (Pa.s), and g is the acceleration due to gravity (m/s²).

- Heat transfer in fluid: the temperature distribution of the liquid manure inside the digesters is governed by the energy equation, given by equation (3).

$$\rho C_p \frac{\partial T}{\partial t} + \rho C_p u \cdot \nabla T + \nabla \cdot (-k \nabla T) = Q \quad (3)$$

T is the fluid temperature (°K), C_p is the fluid specific heat (J/kg.K), k is the fluid thermal conductivity (W/m.K), and Q is the chemical reaction heat (heat source) (W).

- Transport of diluted species: the mole fraction of each species c_i (mol/m³) is calculated using the species transport equation, given by equation (4).

$$\frac{\partial c_i}{\partial t} + \nabla \cdot (-D_i \nabla c_i) + u \cdot \nabla c_i = R_i \quad (4)$$

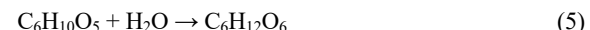
D_i is the diffusion coefficient for species i (m²/s), and R_i is the reaction rate of species i by the chemical reaction (mol/m³.s).

The physical properties of all the species can be obtained from (Yaws 2003).

2.4 Chemical Reaction Equations

AD involves four natural biological processes, represented chemically by the following chemical reaction equations, which are used to calculate the reaction rates and the species concentrations.

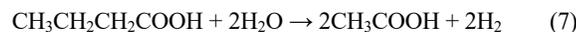
- Hydrolysis: cow manure is regarded as a carbohydrate and hydrolysis is used to reduce the manure to glucose (James N. 2019), as described by the chemical reaction equation (5) (Xiao et al. 2019).



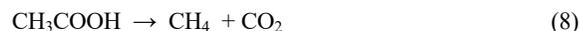
- Acidogenesis: the glucose is converted into butyric acid, as given by the chemical reaction equation (6) (Yuan et al. 2014).



- Acetogenesis: the butyric acid is degraded into acetic acid, as represented by the chemical reaction equation (7) (Zarei et al. 2021).



- Methanogenesis: methane and carbon dioxide are formed from acetic acid, as given by equation (8) (Anukam et al. 2019).



2.5 Reaction Rate and Heat Source Modelling

- The rate of reaction can be calculated using equation (9):

$$r_j = k_j^f \prod_{i \in react} c_i^{-v_{ij}} \quad (9)$$

where C_j is the concentration of species (mol/m³), v_{ij} is the stoichiometric coefficient, and k_j^f is the forward reaction

rate constant (s^{-1}) and can be computed using the Arrhenius expression, as shown by equation (10) (DaCosta and Fan 2012).

$$k^f = A^f \left(\frac{T}{T_{ref}}\right)^{n^f} \exp\left(\frac{-E^f}{R_g T}\right) \quad (10)$$

where A^f is the forward frequency factor (s^{-1}), n^f is the forward temperature exponent, R_g is the ideal gas constant, and E^f is the forward activation energy (J/mol), all of which can be obtained from Azargoshasb et al. (2015), Yaws (2003) and He et al. (2021).

- The heat source in the energy equation represents the heat of the chemical reaction and can be determined from equation (11).

$$Q_j = -r_j H_j \quad (11)$$

H_j is the enthalpy of the reaction for species j and can be computed from equation (12).

$$H_j = \sum_i \epsilon_{prod} \nu_{ij} h_i - \sum_i \epsilon_{react} (-\nu_{ij}) h_i \quad (12)$$

2.6 Boundary Conditions

All the walls, bases, and extended surfaces of the digesters are not slipped (fixed wall), insulated (adiabatic), and there is no flux in the concentration of the species. The cover (top) of the digesters is the open boundary for velocity, temperature, and concentration.

3. NUMERICAL IMPLEMENTATION

3.1 Mesh Analysis

The mesh independence analysis was achieved for the four digesters (D1, D2, D3, and D4). The user-controlled mesh sequence type was predominantly triangular, and the corner refinement scaling factor was 0.25, with the minimum angle between boundaries set at 240° . There were two boundary layers, with a 1.2 stretching factor, a 2×10^{-5} thickness, and trimmed sharp corners with a two-layer decrement. The size of the elements calibrated for fluid dynamics was predefined as extremely fine, with a 0.05 growth rate, a 0.2 curvature factor, and one narrow region resolution.

The number of elements was 102560, 109789, 109155, and 107887, while the average element qualities were 0.9653, 0.9517, 0.9516, and 0.9528 for the digesters D1, D2, D3, and D4, respectively. The mesh element quality is typically a number between 0 and 1, with 0.0 denoting a degenerated element and 1.0 denoting the best possible element. ("COMSOL Multiphysics Reference Manual", 1998). Table (1) and Fig. 3 show the elements and quality of each digester. The mesh

D1		D2		D3		D3	
Mesh quality	NO. of Elements						
0.8206	1417	0.817	1787	0.8298	2278	0.8122	2726
0.8294	1843	0.8387	2337	0.8392	2896	0.8307	3535
0.8646	2294	0.8633	2760	0.8614	3340	0.8445	3954
0.877	2721	0.8805	3159	0.8821	3735	0.8632	4356
0.8914	3868	0.8926	4209	0.8913	4663	0.8862	5251
0.8734	5311	0.904	5406	0.8982	5924	0.8869	6198
0.9321	7248	0.9296	7249	0.9259	7573	0.9252	7765
0.9594	27904	0.9352	30090	0.9343	29960	0.933	29782
0.9653	102560	0.9517	109789	0.9516	109155	0.9528	107887
0.9598	136378	0.9489	144256	0.948	143320	0.9492	142002
0.9525	189425	0.947	196437	0.9478	194623	0.9461	193085
0.9501	275646	0.9428	283065	0.9511	277915	0.9251	272969

configuration for all digesters is shown in Fig. 4.

Table 1 Quality of the elements.

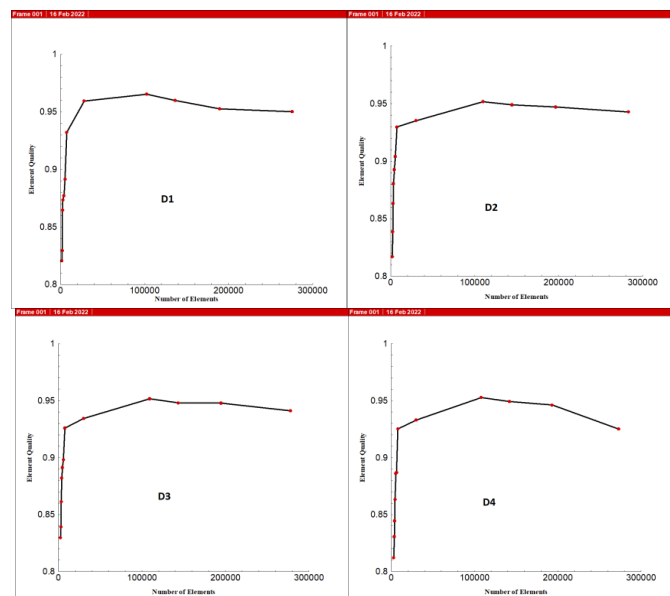


Fig. 3 The stability of the mesh.

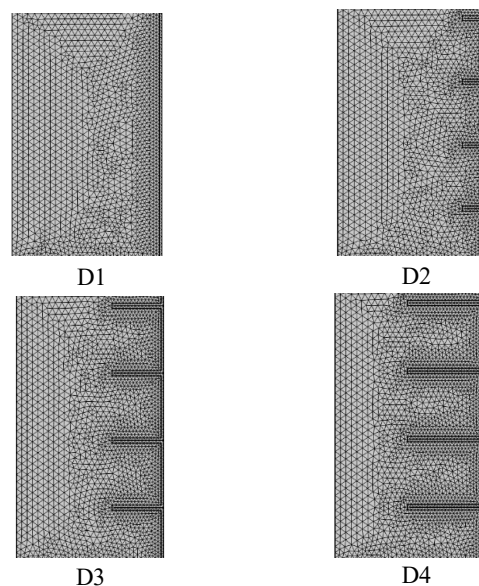


Fig. 4 The configuration of the meshes for the four digesters.

3.2 Numerical Scheme

The governing equations were solved using the finite element method, and all variables were solved using linear discretization. One study with two time-dependent steps was applied to solve each of the four AD processes of the model. Non-isothermal flow multiphysics, which involved fluid flow (the momentum equation) and heat transfer (the energy equation), was solved in the first time-dependent step, while the chemistry (the chemical reactions) and transport for the diluted species equations were solved in the second step. The velocity, pressure, and

temperature vectors coupled the momentum and energy equations. The first step of the study solves these equations, and the variables are updated, while the transport of the diluted species is solved in the second step of the study using the updated variables values from the first step. From this, the solution of the first process of AD is completed. The final updated variables value under the time-dependent (0 to 7 days) one day step time for the first process (hydrolysis) were represented as the initial values from (7 to 14 days) time-dependent for studies of the second process (acidogenesis). The final solution of the second process is initial values for the third process (acetogenesis) of (14 to 21 days) time depended while the time depended on the fourth process (Methanogenesis) of the AD starts from 21 days, which final solution of the third process, to 30 days also with one day step.

Each study's time-dependent solver applied user controller tolerance with 0.001 relative tolerance and nonlinear controller time stepping with backward Euler initialization. It was also fully coupled with the PARDISO algorithm using the constant Newton nonlinear method and the Jacobian update once per time step. Anderson's nonlinear acceleration method for each study should be used to accelerate convergence and reduce the solution time.

4. RESULTS AND DISCUSSION

Four series runs for the four AD processes were performed using CFD analysis to simulate the 3D axisymmetric velocity vector, temperature, and transport of species adding to the chemical reaction for each process using the commercial COMSOL 5.5 Multiphysics software. The runs were repeated for each geometry of the batch reactor to investigate the extended surfaces' influence on the AD performance's heat and mass transfer values. The results simulated four processes of anaerobic digestion. Each process is completed by another and takes seven days, except for the final process, which takes nine days. Finally, the results of the time final processes were discussed.

The results in this work describe the behaviour of the velocity vector for all AD processes for all the geometries of the half (3D axisymmetric) batch reactors, as shown in Fig. 5. The velocity distribution inside the digester results from the heat from the chemical reactions on the inside surfaces, resulting in natural convection currents. Since the reactions are either endothermic or exothermic, the heat is mapped as either heat generation or absorption on the map. From Fig. 5, the path of the velocity vector went from down to up for the hydrolysis and acidogenesis processes for digesters. However, the path flipped in the acetogenesis and methanogenesis processes, going from up to down. This occurs because the chemical reaction is exothermic for first two processes, leading to heat transfer to the inside of the reactor. For the two final processes, the chemical reaction is endothermic, leading to heat being absorbed by the reactor. The above applies to the eddies between the extended surfaces, which appear in the D3 and D4.

Fig. 6 illustrates the temperature distribution for all the AD processes for all the batch reactor geometries. From the figure, it can be seen that the temperature increased by a percent 1.6 % from D1 to D4 with the increasing extended surfaces because of the surface of the chemical reactions increment. These increments were achieved for the hydrolysis and acidogenesis processes via exothermic chemical reactions. However, the chemical reactions were endothermic for the acetogenesis and methanogenesis processes, so the temperature behaviour decreased from D1 to D4 with the extended surfaces reducing due to the decrement in the surfaces of the chemical reaction.

The first process, the hydrolysis of AD, at seven days for the four digesters' geometries is illustrated in Fig. 7. The profile of the reactant carbohydrate molar concentration drops from the boundary layers of the walls and the extended surfaces of digesters while the product glucose molar concentration profile rises from the boundary layers, as shown in Fig. 7. From Fig. 7, it was observed that the drop rate of the carbohydrate species and the rising rate of the glucose species

increased by a percentage of 20 % from D1 to D4 with the increase in the extended surfaces due to the chemical reaction area increment.

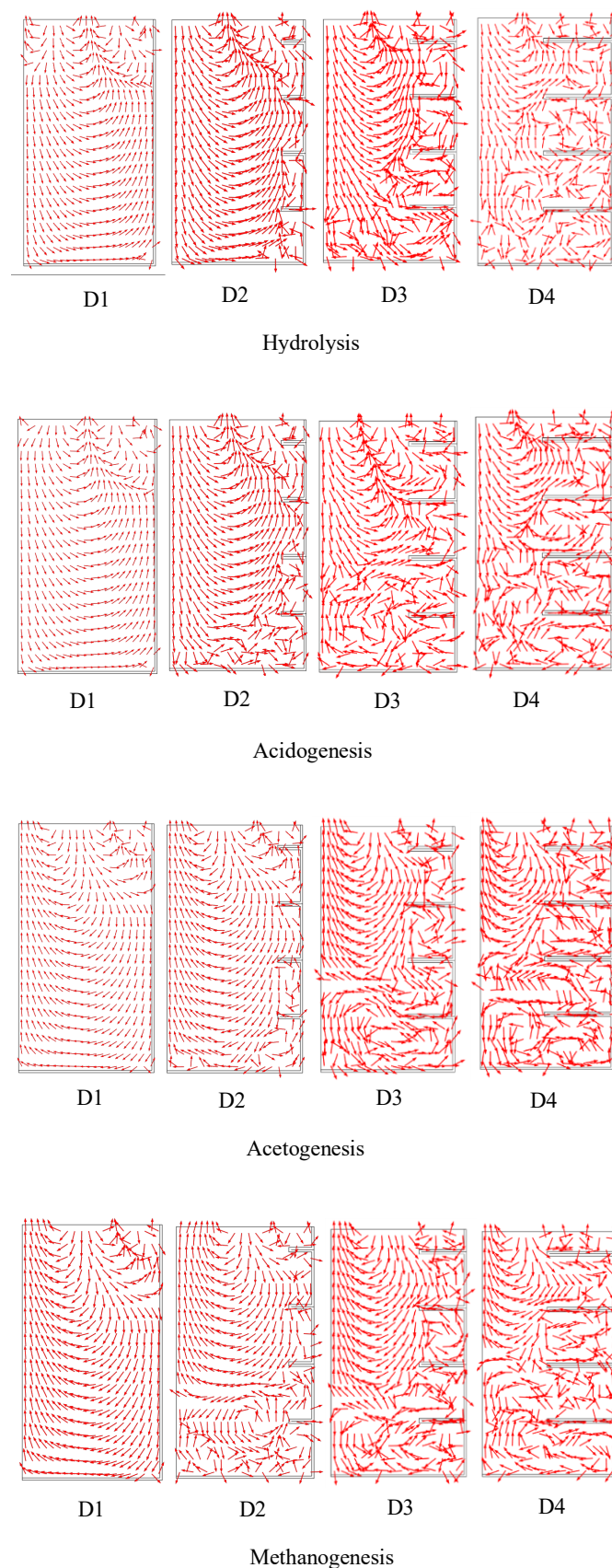


Fig. 5 The velocity vector distribution for the four AD processes for four batch reactors geometries 3D axisymmetric.

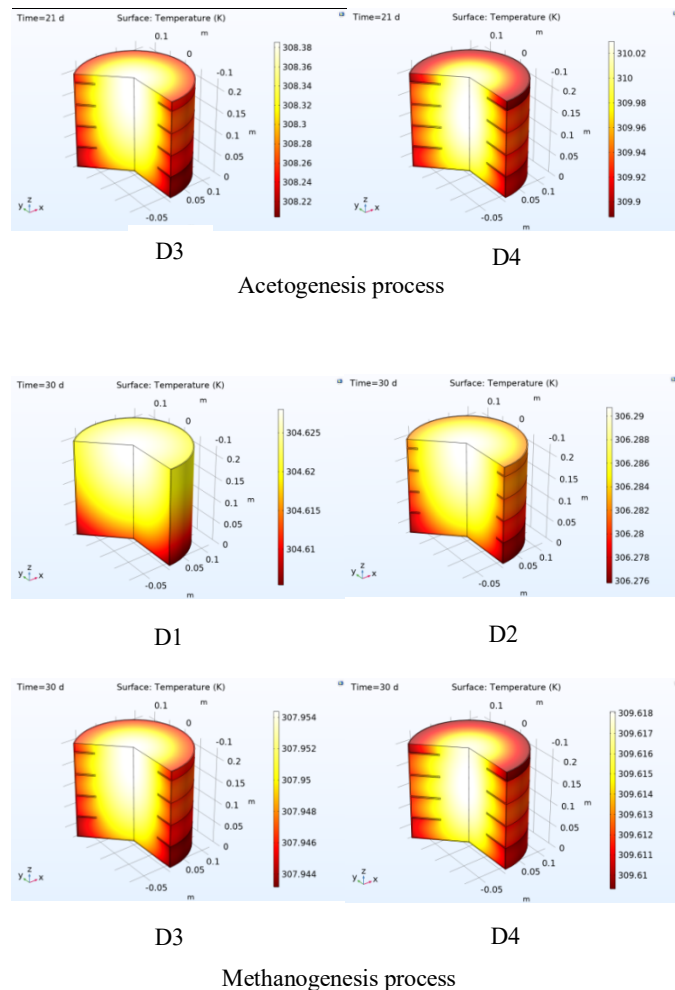
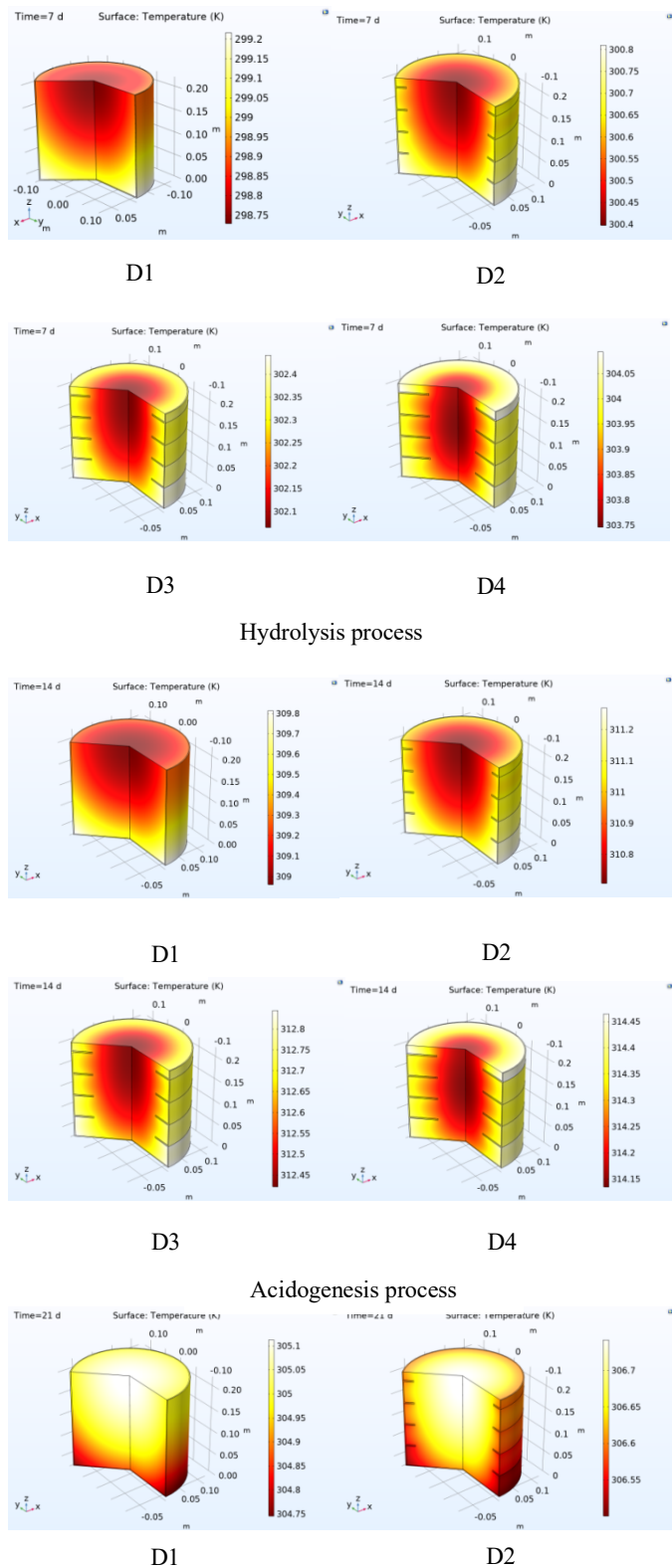
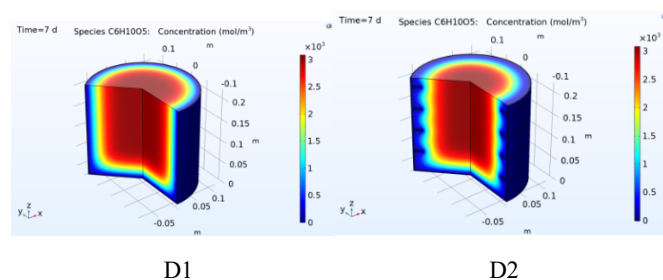


Fig. 6 The temperature distribution for the four processes of AD for four batch reactors' geometries.

Figs. 8, 9, and 10 represent the species of the reactant and the product behaviour for all the digesters for the acidogenesis, acetogenesis, and methanogenesis processes at 14, 21, and 30 days of anaerobic digestion, respectively. Where the species profiles of the reactants of residual processes (the glucose, butyrate, and acetate for the acidogenesis, acetogenesis, and methanogenesis processes, respectively) are dropped from the boundary layers, but the product species profiles of these processes (the butyrate, acetate, and methane for the acidogenesis, acetogenesis and methanogenesis processes, respectively) arise from boundary layers. The drop and rise rates of the species reactants and products for AD's acidogenesis, acetogenesis, and methanogenesis processes depended on the chemical reaction surface area. The extended surfaces of the digesters increased from D1 to D4, leading to the species molar concentration increments of 49 %, 50 % and 78 % for the glucose, butyrate, and acetate products for the acidogenesis, acetogenesis, and methanogenesis processes, respectively shown in Figs (8), (9), and (10).



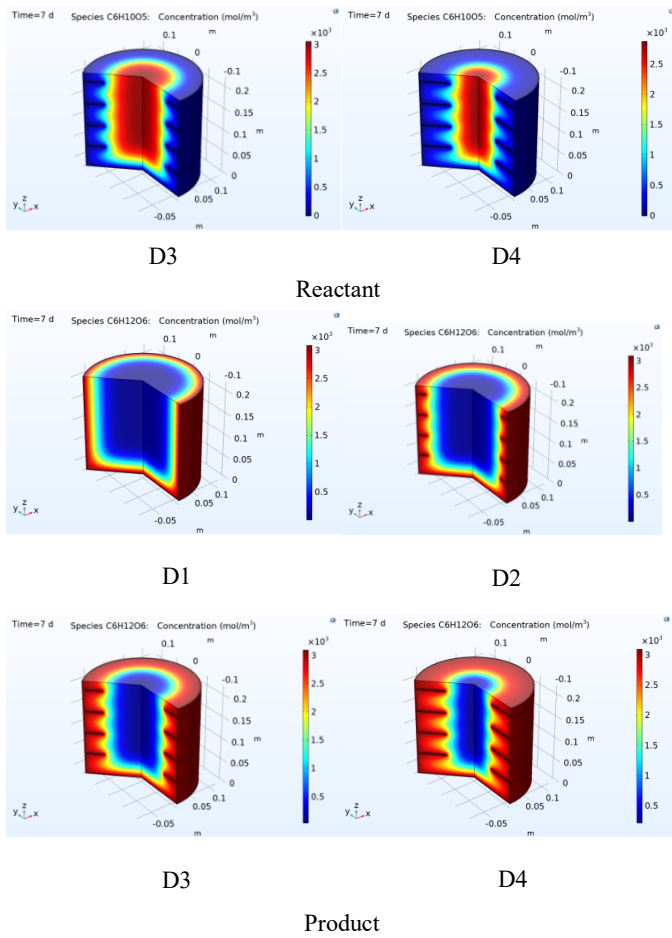


Fig. 7 The molar carbohydrate and glucose concentration behaviour for four digesters at the final hydrolysis process of AD at seven days.

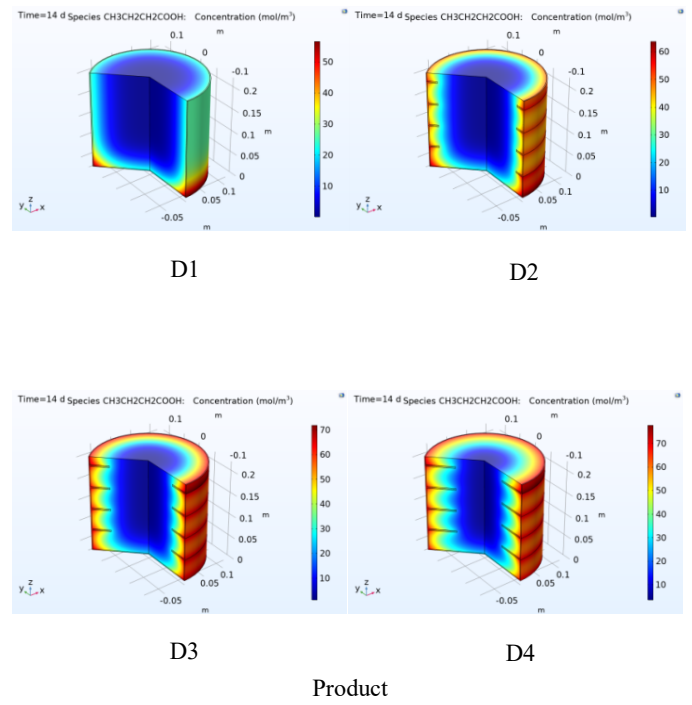
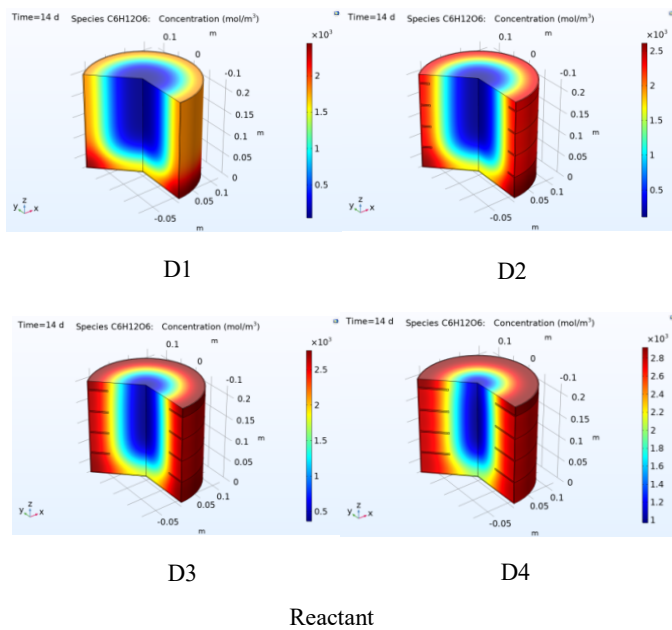
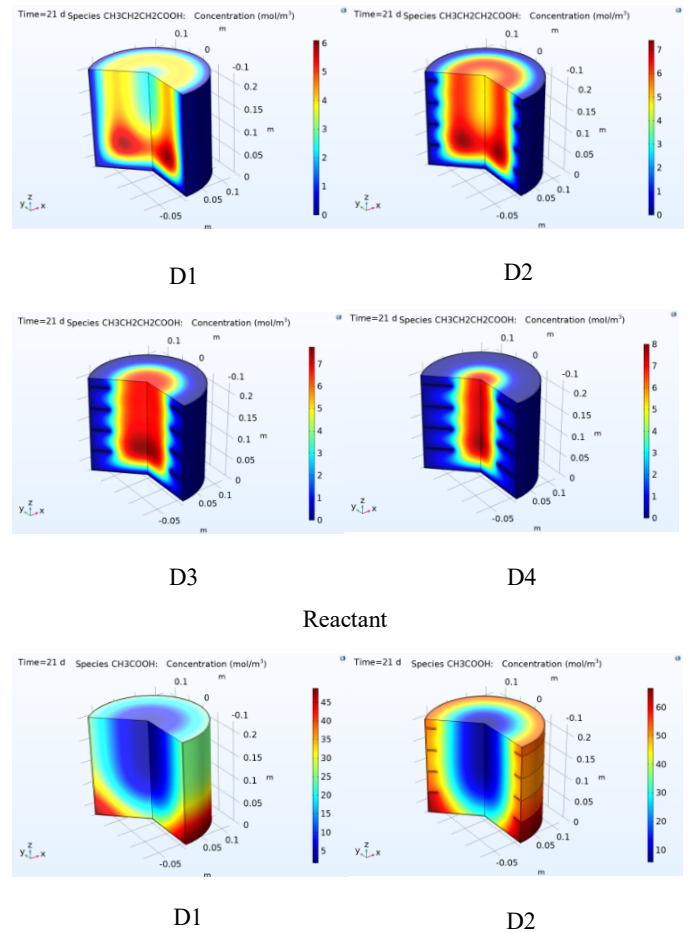


Fig. 8 The molar concentration profile of glucose and butyrate for the four digesters at the final acidogenesis process of AD at 14 days.



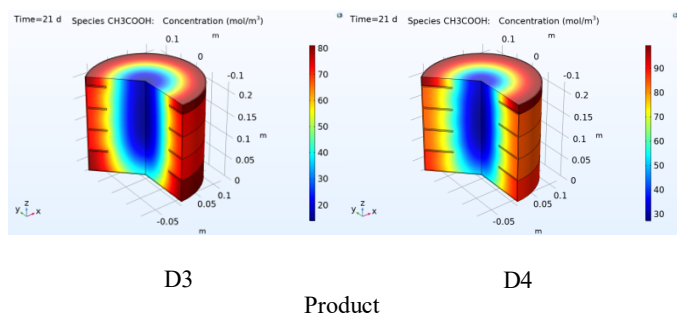


Fig. 9 The molar concentration profile of butyrate and acetate for the four digesters at the final acetogenesis process of AD at 21 days.

4.1 Validation of the Simulation Results

Due to the novelty of this work, the model cannot be verified by the current literature models. Therefore, the validation for the simulation results does not exist, and the validation of the sub-model of the D1 numerical results can be performed individually with experimental works.

The mole concentration average of the butyric acid for the acidogenesis and acetogenesis processes of AD was validated with the experimental work of Li, Jha, and Bajracharya (2014), which used cow dung as substrate with a 2.5 L effective volume batch anaerobic digester for 63 days under a mesophilic temperature of (35 °C) with the mean absolute percent error (MAPE 5.8 %), as shown in Fig. 11-a. In comparison, the average acetic acid mole concentration, shown in Fig. 11-b, of the acetogenesis process of AD, compared with Komemoto et al. (2009), which used food waste as substrate, had a 2L effective volume batch digester for 22 days under mesophilic temperature (35 °C) and an 8.4 % MAPE between them.

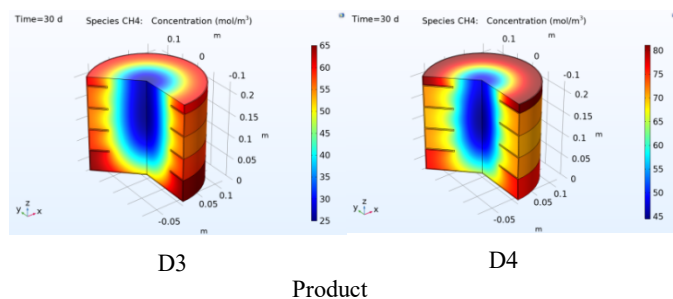
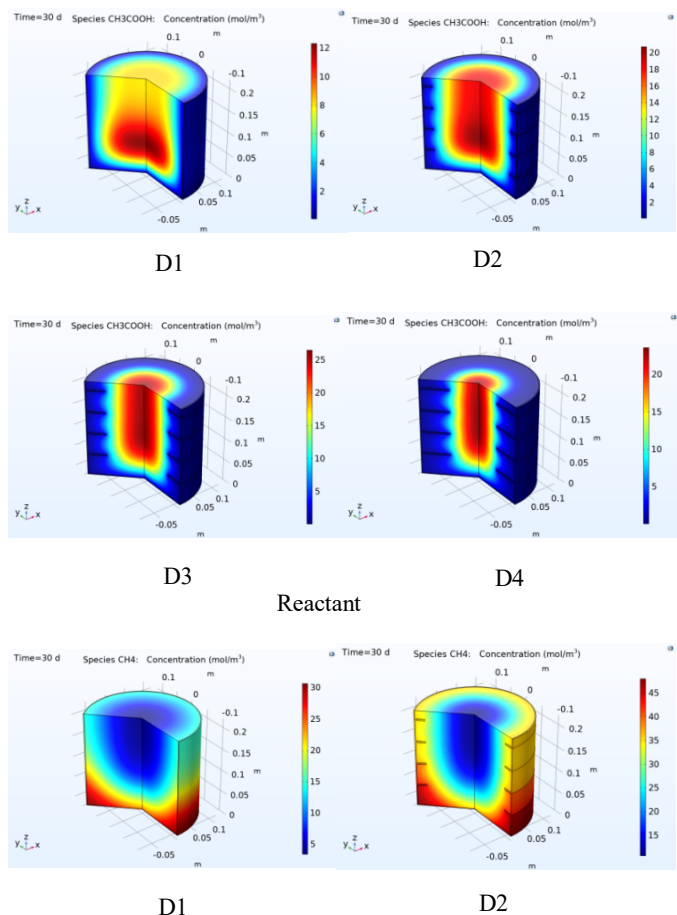
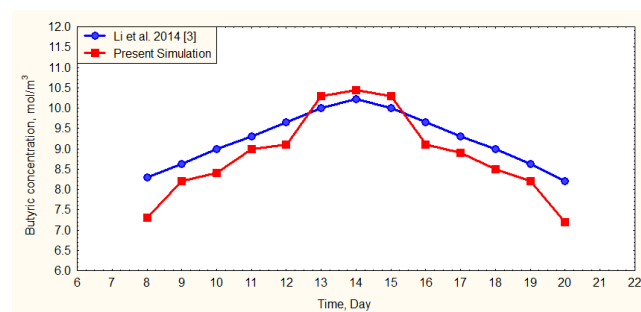
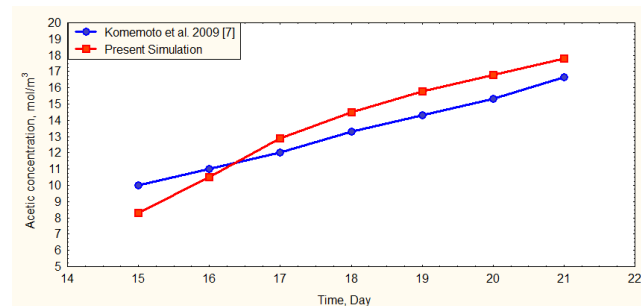


Fig. 10 The molar concentration profiles of acetate and methane for the four digesters at the final methanogenesis process of AD at 30 days.

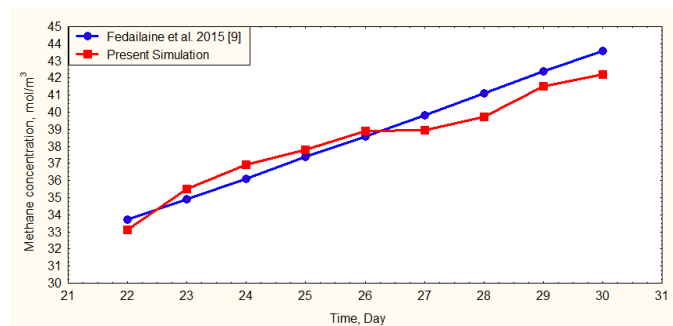
Fig. 11-c showed 1.9 % MAPE of the comparison of methane mole concentration average evolution against the modelling of Fedailaine et al. (2015), which used organic waste as substrate had a 10 L volume digester for 80 days under mesophilic conditions at the methanogenesis process of anaerobic digestion.



(a) Validation of butyric mole concentration against the Li, Jha, and Bajracharya (2014) experimental work.



(b) Validation of acetic mole concentration against the Komemoto et al. (2009) experimental work.



(c) Validation of methane mole concentration against the Fedailaine et al. (2015) modelling

Fig. 11 Comparison of the concentration distribution between the simulation results against experimental literature works.

5. CONCLUSIONS

The purpose of this paper is to present the CFD simulation with a chemical reaction model of AD processes to investigate the influence of different horizontal circular extended surface areas inside the batch reactors on AD and methane production performance.

The simulation results show that the manure's velocity distribution inside the digesters depends on the chemical reaction heat that produces natural convection currents. The chemical reaction is either endothermic or exothermic; thus, there is either heat generation or heat absorption. The chemical reactions of AD's hydrolysis and acidogenesis processes are exothermic, while the acetogenesis and methanogenesis processes are endothermic.

The chemical reaction occurs on the surface area and the horizontal circular extended surfaces. The reaction rate and the chemical reaction heat increase as the extended surface area increases, and the heat and all species' behaviour start from surface boundary layers.

The temperature profiles, the reactants' species, and the products for AD processes depend on the extended surface area. Therefore, they are at a minimum for the D1, which had no extended surfaces, and at a maximum for the D4, which had the maximum extended surfaces.

The maximum performance can be obtained from the D4 because the maximum methane molar concentration is obtained due to the maximum surface area. The simulation results are compared to current experimental results and are in good agreement.

CONFLICT OF INTEREST

All authors declare that they have no known competing financial interests or personal relationships that could have appeared to influence the work reported in this paper.

NOMENCLATURE

Abbreviations

AD	Anaerobic Digestion.
CFD	Computation Fluid Dynamics.
MAPE	Mean Absolute Percent Error.
VFA	Volatile fatty acid.

Symbols

A^f	Forward frequency factor, s^{-1}
c	Mole fraction, mol/m^3
C_p	Specific heat, $J/kg.K$
D	Diffusion coefficient, m^2/s
E^f	Activation energy, J/mol
g	Gravity acceleration, m/s^2
h	Enthalpy of reaction, $KJ/Kmol$
k	Thermal conductivity, $W/m.K$
k^f	Forward reaction rate constant, s^{-1}
I	Unit tensor
n^f	Forward temperature exponent
p	Pressure, Pa
Q	Heat source, W
R	Rate of reaction, $mol/m^3.s$
R_g	Ideal gas constant
r	Rate of reaction, $mol/m^3.s$
T	Temperature, K
t	Time, s
u	Velocity, m/s

Greek Symbols

ρ	Density, kg/m^3
μ	Viscosity, Pa.s

ν stoichiometric coefficient

Subscripts

i	Tensor
j	Species
ref	Reference

REFERENCES

- Martínez, A. M., Martínez, T. M., Fajardo, V., Montañana, and Jiménez, P. A. L. 2011. "Modeling Flow inside an Anaerobic Digester by CFD Techniques." *INTERNATIONAL JOURNAL OF ENERGY AND ENVIRONMENT* 2 (6): 963–74. <http://hdl.handle.net/10251/43856>.
- Anukam, A., Mohammadi, A., Naqvi, M., and Granström, K. 2019. "A Review of the Chemistry of Anaerobic Digestion: Methods of Accelerating and Optimizing Process Efficiency." *Processes*. MDPI AG. <https://doi.org/10.3390/PR7080504>.
- Azargoshab, H., Mousavi, S. M., Amani, T., Jafari, A. and Nosrati., M. 2015. "Three-Phase CFD Simulation Coupled with Population Balance Equations of Anaerobic Syntrophic Acidogenesis and Methanogenesis Reactions in a Continuous Stirred Bioreactor." *Journal of Industrial and Engineering Chemistry* 27 (July): 207–17. <https://doi.org/10.1016/j.jiec.2014.12.037>.
- Bridgeman, J. 2012. "Computational Fluid Dynamics Modelling of Sewage Sludge Mixing in an Anaerobic Digester." In *Advances in Engineering Software*, 44:54–62. Elsevier Ltd. <https://doi.org/10.1016/j.advensoft.2011.05.037>.
- Chen, J., Chen, A., Shaw, J., Yeh, C. and Chen, S. 2019. "CFD Simulation of Two-Phase Flows in Anaerobic Digester." In *Journal of Physics: Conference Series*. Vol. 1300. Institute of Physics Publishing. <https://doi.org/10.1088/1742-6596/1300/1/012048>.
- "COMSOL Multiphysics Reference Manual." 1998. www.comsol.com/blogs.
- Conti, F., Saidi, A., and Goldbrunner, M. 2019. "CFD Modelling of Biomass Mixing in Anaerobic Digesters of Biogas Plants." *Environmental and Climate Technologies* 23 (3): 57–69. <https://doi.org/10.2478/rtuct-2019-0079>.
- Dabiri, S., Noorpoor, A., Arfaee, M., Kumar, P., and Rauch, W. 2021. "CFD Modeling of a Stirred Anaerobic Digestion Tank for Evaluating Energy Consumption through Mixing." *Water (Switzerland)* 13 (12). <https://doi.org/10.3390/w13121629>.
- DaCosta, H., and Fan, M. 2012. *Rate Constant Calculation for Thermal Reactions: Methods and Applications*. John Wiley & Sons, Inc., Hoboken, New Jersey.
- Dapelo, D., and Bridgeman, J. 2018. "Assessment of Mixing Quality in Full-Scale, Biogas-Mixed Anaerobic Digestion Using CFD." *Bioresource Technology* 265 (October): 480–89. <https://doi.org/10.1016/j.biortech.2018.06.036>.
- Deng, L., Liu, Y. and Wang, W. 2020. *Biogas Technology*. Springer Nature singapore. <https://doi.org/10.1007/978-981-15-4940-3>.
- Erdiwansyah, E., Mahidin, M., Husni H., Faisal, M., Usman, U., Muhtadin, M., Gani, A. and Mamat, R. 2022. "Modification of Perforated Plate in Fluidized-Bed Combustor To Provide Sufficient Air Supply in the Combustion." *Frontiers in Heat and Mass Transfer* 18: 2018–23. <https://doi.org/10.5098/hmt.18.25>.

Fedailaine, M., Moussi, K., Khitous, M, Abada, S., Saber, M. and Tirichine, N. 2015. "Modeling of the Anaerobic Digestion of Organic Waste for Biogas Production." In *Procedia Computer Science*, 52:730–37. Elsevier B.V. <https://doi.org/10.1016/j.procs.2015.05.086>.

Rodríguez, F., Pérez, J. M. and Romero, L. I. 2013. "Comparison of Mesophilic and Thermophilic Dry Anaerobic Digestion of OFMSW: Kinetic Analysis." *Chemical Engineering Journal* 232 (October): 59–64. <https://doi.org/10.1016/j.cej.2013.07.066>.

He, O., Zhang, Y., Wang, P., Liu, L., Wang, Q., Yang, N., Li, W., Champagne, P. and Yu, H. 2021. "Experimental and Kinetic Study on the Production of Furfural and HMF from Glucose." *Catalysts* 11 (1): 1–13. <https://doi.org/10.3390/catal11010011>.

Ibrahimi, M., Khay, I., El Maakoul, A. and Bakhouya, M. 2021. "Food Waste Treatment through Anaerobic Co-Digestion: Effects of Mixing Intensity on the Thermohydraulic Performance and Methane Production of a Liquid Recirculation Digester." *Process Safety and Environmental Protection* 147 (March): 1171–84. <https://doi.org/10.1016/j.psep.2021.01.027>.

James N., B. 2019. *Carbohydrate Chemistry for Food Scientists*. Third Edit. AACC International. <https://doi.org/10.1016/B978-0-12-812069-9.00001-7>.

Jegade, A. O., Gualtieri, C., Zeeman, G. and Bruning, H.. 2020. "Three-Phase Simulation of the Hydraulic Characteristics of an Optimized Chinese Dome Digester Using COMSOL Multiphysics." *Renewable Energy* 157 (September): 530–44. <https://doi.org/10.1016/j.renene.2020.05.011>.

Kamarád, L., Pohn, S., Bochmann, G. and Harasek, M. 2013. "Determination of Mixing Quality in Biogas Plant Digesters Using Tracer Tests and Computational Fluid Dynamics." *Acta Universitatis Agriculturae et Silviculturae Mendelianae Brunensis* 61 (5): 1269–78. <https://doi.org/10.1118/actaun201361051269>.

Kolbl, S., Tavčer, P. F. and Stres, B. 2017. "Potential for Valorization of Dehydrated Paper Pulp Sludge for Biogas Production: Addition of Selected Hydrolytic Enzymes in Semi-Continuous Anaerobic Digestion Assays." *Energy* 126: 326–34. <https://doi.org/10.1016/j.energy.2017.03.050>.

Komemoto, K., Lim, Y. G., Nagao, N., Onoue, Y., Niwa, C. and Toda, T. 2009. "Effect of Temperature on VFA's and Biogas Production in Anaerobic Solubilization of Food Waste." *Waste Management* 29 (12): 2950–55. <https://doi.org/10.1016/j.wasman.2009.07.011>.

Leonzio, G. 2018. "Study of Mixing Systems and Geometric Configurations for Anaerobic Digesters Using CFD Analysis." *Renewable Energy* 123 (August): 578–89. <https://doi.org/10.1016/j.renene.2018.02.071>.

Li, J., Jha A. K., and Bajracharya, T. R. 2014. "Dry Anaerobic Co-Digestion of Cow Dung with Pig Manure for Methane Production." *Applied Biochemistry and Biotechnology* 173 (6): 1537–52. <https://doi.org/10.1007/s12010-014-0941-z>.

Mao, L., Zhang, J., Dai, Y. and Tong, Y. W. 2019. "Effects of Mixing Time on Methane Production from Anaerobic Co-Digestion of Food Waste and Chicken Manure: Experimental Studies and CFD Analysis." *Bioresour. Technology* 294 (December). <https://doi.org/10.1016/j.biortech.2019.122177>.

Christy, M. P., Gopinath, L. R. and Divya, D. 2014. "A Review on Anaerobic Decomposition and Enhancement of Biogas Production through Enzymes and Microorganisms." *Renewable and Sustainable Energy Reviews* 34: 167–73. <https://doi.org/10.1016/j.rser.2014.03.010>.

Meroney, R. N., and Colorado, P. E. 2009. "CFD Simulation of Mechanical Draft Tube Mixing in Anaerobic Digester Tanks." *Water Research* 43 (4): 1040–50. <https://doi.org/10.1016/j.watres.2008.11.035>.

Mohammadrezaei, R., Zareei, S. and Khazaei, N. B. 2018. "Optimum Mixing Rate in Biogas Reactors: Energy Balance Calculations and Computational Fluid Dynamics Simulation." *Energy* 159 (September): 54–60. <https://doi.org/10.1016/j.energy.2018.06.132>.

Nasir, A., Bala, K. C., Mohammed, S. N., Mohammed, A. and Umar, I. 2015. "Experimental Investigation on the Effects of Digester Size on Biogas Production from Cow Dung." *American Journal of Engineering Research* 4 (1): 181–86. www.ajer.org.

Noonari, A. A., Mahar, R. B., Sahito, A. R. and Brohi, K. M. 2020. "Effects of Isolated Fungal Pretreatment on Bio-Methane Production through the Co-Digestion of Rice Straw and Buffalo Dung." *Energy* 206 (September). <https://doi.org/10.1016/j.energy.2020.118107>.

Ogunwande, G. A. and Akinjobi, A. J. 2017. "Effect of Digester Surface Area on Biogas Yield." *Agricultural Engineering International: CIGR Journal* 19 (3): 64–69. <http://www.cigrjournal.org>.

Patrícia, V. N., Delly, O. F., Márcio, M. A., Joyce, C. C., André, R. P. and Eduardo, M. A. M. 2020. "Computational Fluid Dynamics Simulation of Thermodynamic Behaviour of Tubular Digester." In *IFAC-PapersOnLine*, 53:15829–34. Elsevier B.V. <https://doi.org/10.1016/j.ifacol.2020.12.234>.

Rajput, A. A., Zeshan, and Hassan, M. 2021. "Enhancing Biogas Production through Co-Digestion and Thermal Pretreatment of Wheat Straw and Sunflower Meal." *Renewable Energy* 168 (May): 1–10. <https://doi.org/10.1016/j.renene.2020.11.149>.

Rathaur, R., Dhawane, S. H., Ganguly, A., Mandal, M. K. and Halder, G. 2018. "Methanogenesis of Organic Wastes and Their Blend in Batch Anaerobic Digester: Experimental and Kinetic Study." *Process Safety and Environmental Protection* 113 (January): 413–23. <https://doi.org/10.1016/j.psep.2017.11.014>.

Massoud, R., Winkler, D., Sappl, J., Seiler, L., Meister, M. and Rauch, W. 2019. "A Fully Lagrangian Computational Model for the Integration of Mixing and Biochemical Reactions in Anaerobic Digestion." *Computers and Fluids* 181 (March): 224–35. <https://doi.org/10.1016/j.compfluid.2019.01.024>.

Saini, A. K., Paritosh, K., Singh, A. K. and Vivekanand V. 2021. "CFD Approach for Pumped-Recirculation Mixing Strategy in Wastewater Treatment: Minimizing Power Consumption, Enhancing Resource Recovery in Commercial Anaerobic Digester." *Journal of Water Process Engineering* 40 (April). <https://doi.org/10.1016/j.jwpe.2020.101777>.

Sanchez, S., and Demain, A. L. 2017. *Useful Microbial Enzymes-An Introduction. Biotechnology of Microbial Enzymes: Production, Biocatalysis and Industrial Applications*. Vol. 2017. Elsevier Inc. <https://doi.org/10.1016/B978-0-12-803725-6.00001-7>.

Sawyer, N., Trois, C., Workneh, T., and Okudoh, V. 2019. "An Overview of Biogas Production: Fundamentals, Applications and Future Research." *International Journal of Energy Economics and Policy* 9 (2): 105–16. <https://doi.org/10.32479/ijeep.7375>.

Shen, F., Tian, L., Yuan, H., Pang, Y., Chen, S., Zou, D., Zhu, B., Liu, Y. and Li, X. 2013. "Improving the Mixing Performances of Rice Straw Anaerobic Digestion for Higher Biogas Production by Computational Fluid Dynamics (CFD) Simulation." *Applied*

Biochemistry and Biotechnology 171 (3): 626–42.
<https://doi.org/10.1007/s12010-013-0375-z>.

Terashima, M., Goel, R., Komatsu, K., Yasui, H., Takahashi, H., Li, Y. Y., and Noike, T. 2009. “CFD Simulation of Mixing in Anaerobic Digesters.” *Bioresource Technology* 100 (7): 2228–33.
<https://doi.org/10.1016/j.biortech.2008.07.069>.

Treichel, H., and Fongaro, G. 2019. *Improving Biogas Production*. 9th ed. Springer Nature Switzerland.
https://doi.org/10.1007/978-3-030-10516-7_1.

Wang, P., Wang, H., Qiu, Y., Ren, L. and Jiang, B. 2018. “Microbial Characteristics in Anaerobic Digestion Process of Food Waste for Methane Production—A Review.” *Bioresource Technology* 248: 29–36.
<https://doi.org/10.1016/j.biortech.2017.06.152>.

Wu B., Bibeau E.L., Gebremedhin K.G. 2009. “Three-Dimensional Numerical Simulation Model of Biogas Production for Anaerobic Digesters.” *CANADIAN BIOSYSTEMS ENGINEERING* 51: 8.1-8.7.
[doi:10.13031/2013.20924](https://doi.org/10.13031/2013.20924).

Wu, B. 2010a. “CFD Simulation of Gas and Non-Newtonian Fluid Two-Phase Flow in Anaerobic Digesters.” *Water Research* 44 (13): 3861–74.
<https://doi.org/10.1016/j.watres.2010.04.043>.

Wu, B. 2010b. “Computational Fluid Dynamics Investigation of

Turbulence Models for Non-Newtonian Fluid Flow in Anaerobic Digesters.” *Environmental Science and Technology* 44 (23): 8989–95.
<https://doi.org/10.1021/es1010016>.

Xiao, C., Liao, Q., Fu, Q., Huang, Y., Xia, A., Shen, W., Chen, H. and Zhu, X. 2019. “Exergy Analyses of Biogas Production from Microalgae Biomass via Anaerobic Digestion.” *Bioresource Technology* 289 (October).
<https://doi.org/10.1016/j.biortech.2019.121709>.

Yaws, C. L. 2003. *Yaws’ Handbook of Thermodynamic and Physical Properties of Chemical Compounds*. Knovel. Norwich, NewYork.
<https://app.knovel.com/kn/resources/kpYHTPPCC4/toc>.

Yuan, X. Z., Shi, X. S., Yuan, C. X., Wang, Y. P., Qiu, Y. L., Guo, R. B. and Wang, L. S. 2014. “Modeling Anaerobic Digestion of Blue Algae: Stoichiometric Coefficients of Amino Acids Acidogenesis and Thermodynamics Analysis.” *Water Research* 49 (February): 113–23.
<https://doi.org/10.1016/j.watres.2013.11.015>.

Zarei, S., Mousavi, S. M., Amani, T., Khamfroush, M. and Jafari, A. 2021. “Three-Dimensional CFD Simulation of Anaerobic Reactions in a Continuous Packed-Bed Bioreactor.” *Renewable Energy* 169 (May): 461–72. <http://doi.org/10.1016/j.renene.2021.01.029>

Zobaa, A. F., and Bansal, R. 2011. *Handbook of Renewable Energy Technology*. World Scientific Publishing Co.Pte. Ltd.
<https://www.ptonline.com/articles/how-to-get-better-mfi-results>.